
GLOBAL WELL-POSEDNESS AND NUMERICAL APPROXIMATION OF A COUPLED DARCY-CONVECTION-DIFFUSION SYSTEM WITH EXPONENTIAL NONLINEARITY

Sahil Kundu¹, Amiya K. Pani², Manoranjan Mishra¹

¹Department of Mathematics, Indian Institute of Technology Ropar, Rupnagar, India

²Department of Mathematics, BITS Pilani, K K Birla Goa Campus, Goa, India

24 May, 2024

ABSTRACT

This paper investigates density-driven flow in porous media, focusing on the roles of viscosity contrast, density contrast, and linear adsorption. In this setup, the fluid on top is heavier and more viscous than the fluid below. Under the effect of gravity, this system becomes unstable, and finger-like structures appear. The phenomenon is described mathematically by coupling Darcy's law with a convection-diffusion reaction equation. The nonlinearity in this model arises mainly from the concentration dependence of viscosity and the convective transport term. The existence of a unique pair of weak solutions is shown in both two and three dimensions using the Galerkin approximation method and truncation technique. Moreover, an application of the maximum principle shows non-negativity of the concentration. Additionally, we analyze the long-time behavior of the solution and prove that the concentration converges exponentially to zero in the L^p -norm for all $1 \leq p \leq \infty$ as $t \rightarrow \infty$. To complement the theoretical analysis, we perform numerical simulations based on a pressure formulation. By tracking total kinetic energy and mixing measures over time, we discuss the instability and the mixing efficiency, respectively. The present study reveals that although increasing the density contrast amplifies the total kinetic energy, the marginal impact diminishes with successive increments of density contrast. Similarly, while adsorption acts to suppress mixing, its efficiency in doing so tends to saturate with further increases. These non-linear sensitivities are predicted by our theoretical estimates and confirmed by the numerical simulations.

Keywords : Density fingering · Darcy equation · Miscible flow · Well-posedness · Existence · Uniqueness · Darcy-Brinkman

1 Introduction

The Rayleigh-Taylor instability [25, 29] arises when a heavier fluid pushes into a lighter one within a porous medium. Its development is strongly influenced by the mobility contrast between the fluids, especially when their viscosities differ. This form of instability plays a central role in a variety of practical contexts—for instance, in enhanced oil recovery [1, 16], in carbon dioxide storage and sequestration [26, 13], in the transport of contaminants through groundwater [9, 15], and in chromatographic separation processes [27, 20]. In many of these applications, the solute interacts with the porous matrix, most commonly through adsorption, where part of the solute temporarily binds to the solid structure of the medium [1, 26, 15]. This interaction slows down the solute transport [31] and modifies the movement of concentration fronts. When fluid properties such as density and viscosity changes with solute concentration, adsorption can also indirectly alter the flow, thereby affecting both instability and mixing [24, 12, 23]. These processes can be described mathematically by a coupled system involving fluid flow and solute transport within a porous medium. The governing equations take the form

$$\nabla \cdot \mathbf{u} = 0, \quad \frac{\mu(c_m)}{K} \mathbf{u} = -\nabla p - \rho(c_m) \mathbf{g},$$

where \mathbf{u} denotes the Darcy velocity, p is the pressure, and c_m is the solute concentration in the mobile (fluid) phase. The viscosity $\mu(c_m)$ and density $\rho(c_m)$ depend on the solute concentration. The solute undergoes advection, dispersion, and adsorption–desorption exchange with the solid matrix, governed by

$$\frac{\partial c_m}{\partial t} + \frac{\partial c_s}{\partial t} + \mathbf{u} \cdot \nabla c = D\Delta c + R,$$

where c_s is the adsorbed concentration (static phase), D is the diffusion coefficient, and R represents the reaction term. The appropriate initial and boundary conditions close the system. Details of the model and its assumptions are presented in Section 2.

Several numerical studies have been carried out to examine how density and viscosity contrasts influence density-driven convective flows using the above model [22, 21, 7, 19]. In particular, Manickam et al. [19] investigated fingering instabilities in vertical miscible displacement flows through porous media arising from combined viscosity and density contrasts, employing linear stability analysis along with direct numerical simulations. They perform linear stability analysis by Quasi-Steady-State Approximations and non-linear simulations by Hartley-transform-based pseudospectral method. Their results showed that the flow may develop a potentially stable region followed downstream by a potentially unstable region, or vice versa, depending on the flow velocity and the diffused viscosity and density profiles. This behaviour gives rise to the possibility of so-called “reverse” fingering. Subsequently, [7] reported that the instability is significantly enhanced when a denser, less viscous fluid displaces a lighter, more viscous one in the direction of gravity. Further, [21] studied the coupled effects of viscosity and density gradients on fingering instabilities of a miscible slice in vertical porous media and identified multiple instability regimes characterized by distinct combinations of viscosity and density contrasts.

While these computational studies offer valuable insights, they lack a rigorous discussion on the well-posedness of the underlying mathematical model. In literature, some progress has been made on the well-posedness of miscible displacement in porous media. Foundational work by Amirat et al. [4] established the existence of global weak solutions for compressible miscible flows; however, their analysis was strictly limited to the one-dimensional setting. Furthermore, while Chen et al. [5] developed comprehensive mathematical frameworks for general reservoir models, their results generally rely on the assumption that the fluid properties (such as viscosity) are bounded and globally Lipschitz continuous. This assumption excludes physically critical scenarios where viscosity exhibits strong nonlinear growth. Building on these works, Allali et al. proved the existence and uniqueness of weak solutions for incompressible flows with constant viscosity and permeability [2], while Kundu et al. established well-posedness for a model using the Brinkman equation and a concentration-dependent permeability with constant viscosity [17]. However, to our knowledge, no well-posedness results exist for the coupled system where viscosity depends exponentially on solute concentration. This case poses two distinct mathematical challenges. First, structurally, the Darcy system lacks a velocity diffusion term (Laplacian of velocity), leading to low spatial regularity of the velocity field. The divergence-free condition alone is insufficient to provide control over velocity gradients. Second, the exponential viscosity function is only locally Lipschitz continuous, not globally Lipschitz. This precludes the use of standard uniqueness arguments that rely on global growth conditions. These combined difficulties—low velocity regularity and aggressive nonlinearity create serious obstacles to proving the uniqueness of the solution.

Therefore, the primary goal of this paper is to prove the well-posedness of a model for density-driven miscible flow in porous media that incorporates linear adsorption and concentration-dependent viscosity, under suitable assumptions. To overcome the difficulties posed by the locally Lipschitz viscosity, we employ a truncation argument combined with the maximum principle to establish necessary L^∞ bounds on the concentration. The concept of well-posedness, which is essential for any physically meaningful model, requires the existence, uniqueness, and continuous dependence of solutions on the initial data. Beyond the existence theory, we derive rigorous estimates for the total kinetic energy and the degree of mixing in terms of key parameters, specifically the density contrast, viscosity contrast, and adsorption coefficient. Using these estimates, we predict the effect of these coefficients on the instability and mixing efficiency. To validate these theoretical estimates, we perform numerical simulations using a pressure-based weak formulation [30, 8] in COMSOL Multiphysics. Unlike the commonly used stream function–vorticity approach, is applicable in both two and three dimensions, making it suitable for realistic simulations. We compute the total kinetic energy and the degree of mixing for various parameters, and the results agree closely with our theoretical predictions.

The paper is arranged as follows. Section 2 sets out the governing equations describing density-driven fingering, incorporating viscosity and density contrasts, as well as adsorption effects. In Section 3, we introduce the notation and recall a few preliminary results for our subsequent use. In Section 4, we prove the existence and uniqueness of weak solutions using the Galerkin method. Section 5 focuses on long-time behaviour. Section 6 explains the numerical approach adopted in COMSOL and illustrates how different parameters influence the behavior of the solution. Finally, Section 7, concludes the paper with a brief summary and a discussion of possible extensions of this work.

2 Mathematical Model

We consider the flow of a miscible solute–solvent mixture in a saturated porous medium occupying a bounded Lipschitz domain $\Omega \subset \mathbb{R}^d$ ($d = 2, 3$) with boundary $\partial\Omega$, over the time interval $(0, \infty)$. The flow is assumed to be governed by the Darcy's law, and the solute concentration evolves according to a convection–diffusion–adsorption equation. Under the assumption of local equilibrium between the mobile and adsorbed phases, the adsorbed concentration c_s satisfies the linear isotherm relation $c_s = k c_m$, where k denotes the adsorption coefficient. For convenience in the notation, we denote the concentration in the mobile phase c_m by c . With this assumption, the following system of equations governs the dynamics of the flow.

$$\nabla \cdot \mathbf{u} = 0 \quad \text{in } (0, \infty) \times \Omega, \quad (1a)$$

$$\frac{\mu(c)}{K} \mathbf{u} = -\nabla p - \rho(c) \mathbf{g} \quad \text{in } (0, \infty) \times \Omega, \quad (1b)$$

$$(1+k) \frac{\partial c}{\partial t} + \nabla \cdot (c \mathbf{u}) = D \Delta c - \kappa c \quad \text{in } (0, \infty) \times \Omega. \quad (1c)$$

In the above system, $\mathbf{g}(\mathbf{x})$ denotes the gravity vector and $k(\mathbf{x})$ the spatially varying reaction rate. Throughout the analysis, we assume that $\mathbf{g} \in \mathbf{L}^\infty(\Omega)$ and that there exist positive constant κ_1 such that $\kappa(\mathbf{x}) \geq \kappa_1$ for almost every $\mathbf{x} \in \Omega$. The fluid density [3] and dynamic viscosity are assumed to depend on the solute concentration through the following relations:

$$\rho(c) = 1 + \alpha c, \quad \mu(c) = \exp(R c), \quad (1d)$$

where parameters $\alpha > 0$ and $R > 0$ are the density and viscosity contrast coefficients, reflecting the sensitivity of fluid properties to concentration variations. The system is supplemented with no-flux boundary conditions:

$$\mathbf{u} \cdot \boldsymbol{\nu} = 0, \quad \nabla c \cdot \boldsymbol{\nu} = 0 \quad \text{on } (0, \infty) \times \partial\Omega, \quad (1e)$$

and the initial concentration distribution at $t = 0$ is prescribed by:

$$c(0, \mathbf{x}) = c_0(\mathbf{x}) \quad \text{for } \mathbf{x} \in \Omega. \quad (1f)$$

We assume the initial data is bounded and nonnegative:

$$0 \leq c_0(\mathbf{x}) \leq M_2 \quad \text{for } \mathbf{x} \in \Omega, \quad (1g)$$

where M_2 are non-negative constants.

3 Preliminaries and Concept of Weak Solution

In this section, we introduce the standard notation and recall certain well-known analytical results that will be used throughout the paper. Let $\Omega \subset \mathbb{R}^d$ (with $d = 2$ or 3) be a bounded domain with lipschitz boundary. The Sobolev spaces $W^{k,p}(\Omega)$ and $H^k(\Omega)$ are understood in the usual sense, endowed with their standard norms. The notation (\cdot, \cdot) denotes the standard inner product in both $L^2(\Omega)$ and $(L^2(\Omega))^d$. Similarly, $\|\cdot\|_{L^2}$ denotes the standard norm in these spaces. Let

$$\begin{aligned} \mathbf{H}_0(\text{div}; \Omega) &:= \left\{ \mathbf{v} \in (L^2(\Omega))^d \mid \nabla \cdot \mathbf{v} \in L^2(\Omega), \mathbf{v} \cdot \boldsymbol{\nu} = 0 \text{ on } \partial\Omega \right\}, \\ \mathbf{H}(\Omega) &:= \left\{ \mathbf{v} \in \mathbf{H}_0(\text{div}; \Omega) \mid \nabla \cdot \mathbf{v} = 0 \text{ a.e. in } \Omega \right\}, \end{aligned}$$

where $\boldsymbol{\nu}$ denotes the outward unit normal vector. For any Banach space Y with norm $\|\cdot\|_Y$, we define the Bochner spaces:

$$L^p(a, b; Y) := \left\{ \phi : [a, b] \rightarrow Y : \|\phi\|_{L^p(a, b; Y)} = \left(\int_a^b \|\phi\|_Y^p dt \right)^{\frac{1}{p}} < \infty \right\} \text{ for } 1 \leq p < \infty,$$

and

$$L^\infty(a, b; Y) := \left\{ \phi : [a, b] \rightarrow Y : \|\phi\|_{L^\infty(a, b; Y)} = \text{ess sup}_{[a, b]} \|\phi\|_Y < \infty \right\}.$$

Throughout this manuscript, $M \in [0, \infty)$ will denote a generic, context-dependent constant, whose value may change from line to line.

Theorem 3.1 (Gagliardo–Nirenberg, cf. [28, Lemma 1], [10, Lemma 1.1]). *If $\Omega \subset \mathbb{R}^d$ ($d = 2, 3$) is a domain, then for any $\phi \in H^1(\Omega)$ there exists a constant $M > 0$ depending only on Ω such that the following inequality holds when $d = 2$*

$$\|\phi\|_{L^4} \leq M \|\phi\|_{L^2}^{1/2} \|\phi\|_{H^1}^{1/2},$$

and for $d = 3$, the inequality

$$\|\phi\|_{L^4} \leq M \|\phi\|_{L^2}^{1/4} \|\phi\|_{H^1}^{3/4} \quad \text{holds.}$$

Young's inequality: Let p, q be positive real numbers satisfying $\frac{1}{p} + \frac{1}{q} = 1$, and a, b are non-negative real numbers. Then for any given $\epsilon > 0$, there exist a non-negative constant say M_ϵ such that

$$ab \leq \epsilon a^p + M_\epsilon b^q.$$

Below, we discuss the concept of weak solution of the system (1).

Definition 3.1 (Weak Solution of System (1)). *A pair (c, \mathbf{u}) is said to be a weak solution of the system (1a)–(1g) if the following conditions are satisfied:*

(i) *The solution possesses the global regularity*

$$c \in L^\infty(0, \infty; L^\infty(\Omega)) \cap L^2(0, \infty; H^1(\Omega)), \quad \mathbf{u} \in L^2(0, \infty; \mathbf{H}) \cap L^2(0, \infty; \mathbf{L}^p(\Omega)),$$

and the local-in-time regularity for any finite $T > 0$,

$$\frac{\partial c}{\partial t} \in L^r(0, T; (H^1(\Omega))^*),$$

where the exponents r and p are defined as:

$$r = \begin{cases} 2, & d = 2, \\ \frac{4}{3}, & d = 3, \end{cases} \quad \text{and} \quad p = \begin{cases} [2, \infty), & d = 2, \\ [2, 6], & d = 3. \end{cases}$$

(ii) *The initial condition $c(0, \mathbf{x}) = c_0(\mathbf{x})$ from (1f) is satisfied in $L^2(\Omega)$.*

(iii) *For almost every $t \in (0, \infty)$, the following identities hold:*

$$\left(\frac{\mu(c)}{K} \mathbf{u}(t), \mathbf{v} \right) + ((1 + \alpha c(t)) \mathbf{g}, \mathbf{v}) = 0, \quad \forall \mathbf{v} \in \mathbf{H}(\Omega), \quad (2)$$

$$(1 + k) \left\langle \frac{\partial c(t)}{\partial t}, \phi \right\rangle + (c(t) \mathbf{u}(t), \nabla \phi) + D(\nabla c(t), \nabla \phi) + (\kappa c, \phi) = 0, \quad \forall \phi \in H^1(\Omega). \quad (3)$$

4 Existence and uniqueness results for the weak solution

This section deals with existence of a unique weak solution to the problem (1a)–(1f).

Below, we state the main theorem whose proof can be established after deriving some *a priori* bounds.

Theorem 4.1. *For any initial data $c_0 \in L^2(\Omega)$, there exists a solution (c, \mathbf{u}) to the system (1a)–(1f), in the sense of definition 3.1.*

For the proof of the Theorem 4.1, we adopt the following strategy:

- **Strategy-I:** Due to exponential nonlinearity, we introduce the ℓ -approximate problem based on the truncation technique whose solution pair may be referred to as $\{(c_\ell, \mathbf{u}_\ell)\}$.
- **Strategy-II:** To this approximate problem, apply the Bubnov-Galerkin method, which provides finite dimensional approximation, say $\{(c_{\ell,n}, \mathbf{u}_{\ell,n})\}$ to the truncated system.
- **Strategy-III:** We then derive uniform bounds of the sequence $\{(c_{\ell,n}, \mathbf{u}_{\ell,n})\}$ with respect to n . Using standard weak or weak* compactness arguments, and passing the limit as $n \rightarrow \infty$, we prove convergence of $(c_{\ell,n}, \mathbf{u}_{\ell,n})$ to $(c_\ell, \mathbf{u}_\ell)$.
- **Strategy-IV:** (Passing limit as $\ell \rightarrow \infty$) One of the crucial step is to show the nonnegativity of c_ℓ by using weak maximum principle. finally, we pass the limit $\ell \rightarrow \infty$ to complete the rest of the proof.

4.1 Truncation and Bubnov-Galerkin approximation.

Since exponential nonlinearity is involved in the viscosity term μ , we use the following truncation technique.

We now define the truncated viscosity $\tilde{\mu}(s)$, which is based on a fixed level $\ell > 0$ as

$$\tilde{\mu}(s) = \begin{cases} e^{R\ell} & \text{if } s > \ell, \\ e^{Rs} & \text{if } -\ell \leq s \leq \ell, \\ e^{-R\ell} & \text{if } s < -\ell. \end{cases} \quad (4)$$

Therefore, we define ℓ -approximation $(c_\ell, \mathbf{u}_\ell)$ of the system (2)-(3) as

$$\left(\frac{\tilde{\mu}(c_\ell)}{K} \mathbf{u}_\ell(t), \mathbf{v} \right) + ((1 + \alpha c_\ell(t)) \mathbf{g}, \mathbf{v}) = 0, \quad \forall \mathbf{v} \in \mathbf{H}(\Omega), \quad (5)$$

$$(1 + k) \left\langle \frac{\partial c_\ell(t)}{\partial t}, \phi \right\rangle + (c_\ell(t) \mathbf{u}_\ell(t), \nabla \phi) + D(\nabla c_\ell(t), \nabla \phi) + (\kappa c_\ell, \phi) = 0, \quad \forall \phi \in H^1(\Omega). \quad (6)$$

In fact, we first prove the existence of a weak pair of solution $(c_\ell, \mathbf{u}_\ell)$ in the sense of definition 3.1 using Bubnov-Galerkin method.

Define finite-dimensional subspaces $W_n \subset H^1(\Omega)$ and $\mathbf{H}_n \subset \mathbf{H}(\Omega) \cap \mathbf{L}^p(\Omega)$, respectively as $W_n = \text{span}\{w_1, \dots, w_n\}$ and $\mathbf{H}_n = \text{span}\{z_1, \dots, z_n\}$. Now seek approximate solutions $\mathbf{u}_{\ell,n} : [0, \infty) \rightarrow \mathbf{H}_n$ and $c_{\ell,n} : [0, \infty) \rightarrow W_n$ of the form

$$c_{\ell,n}(t) = \sum_{i=1}^n \beta_i^n(t) w_i, \quad \mathbf{u}_{\ell,n}(t) = \sum_{i=1}^n \lambda_i^n(t) z_i, \quad (7)$$

such that these satisfy the Galerkin system for almost all $t \in (0, \infty)$

$$\left(\frac{\tilde{\mu}(c_{\ell,n}(t))}{K} \mathbf{u}_{\ell,n}(t), z_j \right) + ((1 + \alpha c_{\ell,n}(t)) \mathbf{g}, z_j) = 0, \quad (8)$$

$$(1 + k) \left\langle \frac{\partial c_{\ell,n}(t)}{\partial t}, w_j \right\rangle + (c_{\ell,n}(t) \mathbf{u}_{\ell,n}(t), \nabla w_j) + D(\nabla c_{\ell,n}(t), \nabla w_j) + (\kappa c_{\ell,n}(t), w_j) = 0, \quad (9)$$

for all $j = 1, \dots, n$. and with initial condition $c_{\ell,n}(0)$ as the n the Fourier coefficient of c_0 defined by

$$c_{\ell,n}(0) = \sum_{j=1}^n (c_0, w_j) w_j.$$

For each fixed truncation level $\ell > 0$, we consider the corresponding Galerkin approximation and denote the approximate solutions by $c_{\ell,n}$ and $\mathbf{u}_{\ell,n}$. The analysis proceeds in two stages: we first pass to the limit as $n \rightarrow \infty$ (for fixed ℓ) to obtain a weak solution (u_ℓ, c_ℓ) of the truncated problem, and then let $\ell \rightarrow \infty$ to recover a weak solution of the original system.

This leads to a system of index one ODEs, and now by (8), one can obtain $\mathbf{u}_{\ell,n}$ in terms of $c_{\ell,n}$. Then, on substitution in the (9), it leads to a system of nonlinear ODEs and an application of the classical Picard–Lindelöf theorem yields the existence and uniqueness of solutions for $t \in (0, t^*)$, for some $t^* > 0$. For applying the continuation of arguments, we need some *a priori* bounds, which are given below.

4.2 *A priori* bounds

Lemma 4.1. *The sequences $\{c_{\ell,n}\}$ and $\{\mathbf{u}_{\ell,n}\}$ are uniformly bounded in $L^2(0, \infty; H^1(\Omega)) \cap L^\infty(0, \infty; L^2(\Omega))$ and $L^2(0, \infty; \mathbf{H}(\Omega)) \cap L^2(0, \infty; \mathbf{L}^p(\Omega))$, for $2 \leq p \leq 6$, respectively.*

Proof. Multiply equation (9) by $\beta_j^n(t)$ and sum over $j = 1, \dots, n$, to obtain

$$\frac{(k+1)}{2} \frac{d}{dt} \|c_{\ell,n}(t)\|_{L^2}^2 + \frac{1}{2} (\mathbf{u}_{\ell,n}(t), \nabla c_n^2(t)) + D\|\nabla c_{\ell,n}(t)\|_{L^2}^2 + \kappa_1 \|c_{\ell,n}(t)\|_{L^2}^2 \leq 0, \quad \text{a.e. on } (0, \infty).$$

The second term vanishes upon utilizing the divergence theorem and the divergence-free condition of $\mathbf{u}_{\ell,n}$. Integrating the resulting equation from 0 to $\tau \in (0, \infty)$, we obtain

$$(k+1)\|c_{\ell,n}(t)\|_{L^2}^2 + 2D \int_0^\tau \|\nabla c_{\ell,n}(t)\|_{L^2}^2 + 2\kappa_1 \int_0^\tau \|c_{\ell,n}(t)\|_{L^2}^2 \leq (k+1)\|c_{\ell,n}(0)\|_{L^2}^2.$$

In the above inequality, using $\|c_{n,\ell}(0)\|_{L^2}^2 \leq \|c_0\|_{L^2}^2$, we observe that $\text{ess sup}_{t \in (0, \infty)} \|c_{\ell,n}(t)\|_{L^2} \leq \|c_0\|_{L^2}$. This observation, together with the above inequality, yields that $c_{\ell,n}(t, \mathbf{x})$ is uniformly bounded in $L^\infty(0, \infty; L^2(\Omega)) \cap L^2(0, \infty; H^1(\Omega))$. Now, using the Sobolev embedding theorems, $\|\varphi\|_{L^p} \leq M\|\varphi\|_{H^1}$, $p \in [1, \infty)$ for $d = 2$, and $p \in [1, 6]$ for $d = 3$. Hence $c_{\ell,n}$ is uniformly bounded in $L^2(0, \infty; L^p(\Omega))$ for any $p \in [1, \infty)$ when $d = 2$, and for any $p \in [1, 6]$ when $d = 3$. Invoking the Gagliardo-Nirenberg interpolation inequality, we have the following estimate for any $t > 0$:

$$\|c_{\ell,n}(t)\|_{L^4} \leq M \|c_{\ell,n}(t)\|_{L^2}^{1-d/4} \|c_{\ell,n}(t)\|_{H^1}^{d/4}.$$

For the case $d = 2$, raising the inequality to the fourth power yields:

$$\|c_{\ell,n}(t)\|_{L^4}^4 \leq M \|c_{\ell,n}(t)\|_{L^2}^2 \|c_{\ell,n}(t)\|_{H^1}^2.$$

Utilizing the established uniform bounds for $c_{\ell,n}$ in $L^\infty(0, \infty; L^2(\Omega))$ and $L^2(0, \infty; H^1(\Omega))$, we deduce that $c_{\ell,n}$ is uniformly bounded in $L^4(0, \infty; L^4(\Omega))$. Similarly, for $d = 3$, raising the interpolation inequality to the power $8/3$ gives:

$$\|c_{\ell,n}(t)\|_{L^4}^{8/3} \leq M \|c_{\ell,n}(t)\|_{L^2}^{2/3} \|c_{\ell,n}(t)\|_{H^1}^2.$$

Again, combining this with the a priori estimates, we conclude that $c_{\ell,n}$ is uniformly bounded in $L^{8/3}(0, \infty; L^4(\Omega))$.

Applying the divergence operator to the Darcy equation (1b) (which holds a.e. in t), we derive the following elliptic equation for the pressure $p_n(t)$:

$$\nabla \cdot \left(\frac{K}{\tilde{\mu}(c_{\ell,n})} \nabla p_n \right) = \nabla \cdot \left(\frac{K}{\tilde{\mu}(c_{\ell,n})} (1 + \alpha c_{\ell,n}) \mathbf{g} \right) \quad \text{in } \Omega. \quad (10)$$

From (4), the coefficient $\frac{K}{\tilde{\mu}(c_{\ell,n})}$ is bounded from below and Lipschitz continuous. We denote the effective force term on the right-hand side by $\mathbf{F}_n = \frac{K}{\tilde{\mu}(c_{\ell,n})} (1 + \alpha c_{\ell,n}) \mathbf{g}$. Since the coefficients are uniformly bounded and Lipschitz continuous, classical elliptic regularity results [11] imply that the pressure gradient satisfies the estimate:

$$\|\nabla p_n(t)\|_{L^p} \leq M \|\mathbf{F}_n(t)\|_{L^p}, \quad \text{for } p \in [2, \infty),$$

where M is a positive constant depending only on d , p , and the domain Ω . Combining this pressure estimate with the original Darcy equation yields the following bound for the velocity:

$$\|\mathbf{u}_{\ell,n}(t)\|_{L^p} \leq M \|\mathbf{F}_n(t)\|_{L^p}, \quad \text{for } p \in [2, \infty). \quad (11)$$

Given the established uniform bounds on $c_{\ell,n}$ and the assumption $\mathbf{g} \in L^\infty(\Omega)$, it follows that the force \mathbf{F}_n , and consequently the velocity $\mathbf{u}_{\ell,n}$, are uniformly bounded in $L^2(0, \infty; L^p(\Omega))$. Here, the range of p is $[2, \infty)$ for $d = 2$ and $[2, 6]$ for $d = 3$. Moreover, the space-time integrability of $c_{\ell,n}$ implies that $\mathbf{u}_{\ell,n}$ is uniformly bounded in $L^r(0, \infty; L^4(\Omega))$, where the exponent is $r = 4$ in two dimensions and $r = 8/3$ in three dimensions. \square

Lemma 4.2. *The sequence of time derivatives $\left\{ \frac{\partial c_{\ell,n}}{\partial t} \right\}$ is uniformly bounded in $L^2(0, T; (H^1(\Omega))^*)$ for $d = 2$ and in $L^{4/3}(0, T; (H^1(\Omega))^*)$ for $d = 3$.*

Proof. We decompose any $\phi \in H^1(\Omega)$ into $\phi = \phi_n + \varphi_n$, using the H^1 -orthogonal projection P_n onto W_n (so $\phi_n \in W_n$ and $\varphi_n \in W_n^\perp$). By construction, $\partial_t c_{\ell,n} \in W_n$, which implies the orthogonality $\langle \partial_t c_{\ell,n}, \varphi_n \rangle_{H^1} = 0$. Thus from equation (9), it follows that:

$$(1+k) \left| \langle \frac{\partial c_{\ell,n}(t)}{\partial t}, \phi \rangle \right| = (1+k) \left| \langle \frac{\partial c_{\ell,n}(t)}{\partial t}, \phi_n \rangle \right| \leq |(c_{\ell,n}(t) \mathbf{u}_{\ell,n}(t), \nabla \phi_n)| + D |(\nabla c_{\ell,n}(t), \nabla \phi_n)| + |(\kappa c_{\ell,n}(t), \phi_n)|,$$

a.e. on $(0, T)$. Utilizing Hölder's inequality on the terms on the right-hand side of the above inequality, we obtain:

$$(1+k) \left| \langle \frac{\partial c_{\ell,n}(t)}{\partial t}, \phi \rangle \right| \leq \|c_{\ell,n}(t) \mathbf{u}_{\ell,n}(t)\|_{L^2} \|\nabla \phi_n\|_{L^2} + D \|\nabla c_{\ell,n}(t)\|_{L^2} \|\nabla \phi_n\|_{L^2} + \|\kappa\|_{L^\infty(\Omega)} \|c_{\ell,n}(t)\|_{L^2} \|\phi_n\|_{L^2},$$

for all $\phi \in H^1(\Omega)$. Again, using Holder's inequality, and $\|\phi_n\|_{L^2} \leq \|\phi\|_{L^2}$, we can write

$$(1+k) \left| \left\langle \frac{\partial c_{\ell,n}(t)}{\partial t}, \phi \right\rangle \right| \leq \|c_{\ell,n}(t)\|_{L^4} \|\mathbf{u}_{\ell,n}(t)\|_{L^4} \|\nabla \phi\|_{L^2} + D \|\nabla c_{\ell,n}(t)\|_{L^2} \|\nabla \phi\|_{L^2} + \|\kappa\|_{L^\infty(\Omega)} \|c_{\ell,n}(t)\|_{L^2} \|\phi\|_{L^2},$$

for all $\phi \in H^1(\Omega)$. Taking the supremum over all $\phi \in H^1(\Omega)$ such that $\|\phi\|_{H^1(\Omega)} \leq 1$ in the above inequality yields:

$$(1+k) \sup_{\phi \in H^1(\Omega), \|\phi\|_{H^1} \leq 1} \left| \left\langle \frac{\partial c_{\ell,n}(t)}{\partial t}, \phi \right\rangle \right| \leq \frac{1}{2} \|c_{\ell,n}(t)\|_{L^4}^2 + \frac{1}{2} \|\mathbf{u}_{\ell,n}(t)\|_{L^4}^2 + D \|\nabla c_{\ell,n}(t)\|_{L^2} + \|\kappa\|_{L^\infty(\Omega)} \|c_{\ell,n}(t)\|_{L^2},$$

a.e. on $(0, T)$. Since each term on the right-hand side of the above inequality uniformly bounded in $L^2(0, T)$ for $d = 2$ and to $L^{4/3}(0, T)$ for $d = 3$, it follows that the sequence $\left\{ \frac{\partial c_{\ell,n}}{\partial t} \right\}$ is uniformly bounded in $L^2(0, T; (H^1(\Omega))^*)$ for $d = 2$, $L^{4/3}(0, T; (H^1(\Omega))^*)$ for $d = 3$. \square

4.3 Passage to limit as $n \rightarrow \infty$.

Lemma 4.3. *Let $\{(c_{\ell,n}, \mathbf{u}_{\ell,n})\}_{n \in \mathbb{N}}$ be the sequence of approximate solutions constructed in subsection 4.1. The limit $(c_\ell, \mathbf{u}_\ell)$ obtained as $n \rightarrow \infty$ is a weak solution to the ℓ -approximate problem defined by (5) and (6).*

Proof. Now, from the lemmas 4.1, and 4.2, we conclude that there exists a positive constant $M > 0$ independent of n , such that

$$\|c_{\ell,n}\|_{L^\infty(0,\infty;L^2(\Omega))}, \|c_{\ell,n}\|_{L^2(0,\infty;H^1(\Omega))}, \|\mathbf{u}_{\ell,n}\|_{L^2(0,\infty;\mathbf{H}(\Omega))}, \left\| \frac{\partial c_{\ell,n}}{\partial t} \right\|_{L^r(0,T;(H^1)^*)} \leq M.$$

Applying the diagonalization argument with the above estimates, we obtain subsequences, which are again labeled by $c_{\ell,n}$ and $\mathbf{u}_{\ell,n}$ and satisfy the following convergence result.

$$\begin{aligned} c_{\ell,n} &\rightharpoonup c_\ell && \text{weakly in } L^2(0, \infty; H^1(\Omega)), \\ \frac{\partial c_{\ell,n}}{\partial t} &\rightharpoonup \frac{\partial c_\ell}{\partial t} && \text{weakly in } L^2(0, T; (H^1(\Omega))^*), \\ \mathbf{u}_{\ell,n} &\rightharpoonup \mathbf{u}_\ell && \text{weakly in } L^2(0, \infty; \mathbf{H}(\Omega)), \end{aligned}$$

as $n \rightarrow \infty$. Applying the Aubin-Lions lemma, we deduce that the sequence of Galerkin solutions $c_{\ell,n}$ is relatively compact in $L^r(0, T; L^2(\Omega))$, where $r = 2$ for $d = 2$ and $r = \frac{4}{3}$ for $d = 3$ for any $T > 0$. Hence, up to a subsequence (still denoted by $c_{\ell,n}$), we obtain strong convergence in $L^r(0, T; L^2(\Omega))$. Furthermore, the Aubin-Lions compactness lemma implies that the limit function satisfies $c_\ell \in C([0, T]; L^2(\Omega))$.

For passing the limit into the equations (8)-(9), we fix an $m \in \mathbb{N}$ such that $m \leq n$. Multiplying the discrete equation (8) by a smooth scalar function $\eta \in C_c^\infty[0, T)$ and integrating over time, we obtain that for any $\mathbf{v} \in \mathbf{H}_m$:

$$\int_0^T \int_\Omega \frac{\tilde{\mu}(c_{\ell,n})}{K} \mathbf{u}_{\ell,n} \cdot \mathbf{v} \eta(t) dx dt + \int_0^T \int_\Omega (1 + \alpha c_{\ell,n}) \mathbf{g} \cdot \mathbf{v} \eta(t) dx dt = 0. \quad (12)$$

We observe that the sequence $\{\tilde{\mu}(c_{\ell,n}) \mathbf{u}_{\ell,n}\}_n$ is uniformly bounded in $L^2(0, T; \mathbf{L}^2(\Omega))$, and therefore there exists a subsequence (still denoted by the same index) and a function $\zeta \in L^2(0, T; \mathbf{L}^2(\Omega))$ such that

$$\tilde{\mu}(c_{\ell,n}) \mathbf{u}_{\ell,n} \rightharpoonup \zeta \quad \text{weakly in } L^2(0, T; \mathbf{L}^2(\Omega)), \quad \text{as } n \rightarrow \infty.$$

As $\tilde{\mu}$, is the Lipschitz function and $c_{\ell,n} \rightarrow c_\ell$ in $L^2(0, T; L^2(\Omega))$, therefore $\tilde{\mu}(c_{\ell,n}) \rightarrow \mu(c_\ell)$ in $L^2(0, T; L^2(\Omega))$ as $n \rightarrow \infty$. Also $\mathbf{u}_{\ell,n} \rightharpoonup \mathbf{u}_\ell$ weakly in $L^2(0, T; \mathbf{L}^2(\Omega))$. Then, utilizing the weak-strong convergence result, we arrive at

$$\frac{\tilde{\mu}(c_{\ell,n})}{K} \mathbf{u}_{\ell,n} \rightharpoonup \frac{\tilde{\mu}(c_\ell)}{K} \mathbf{u}_\ell \quad \text{weakly in } L^1(0, T; \mathbf{L}^1(\Omega)) \text{ as } n \rightarrow \infty.$$

By the uniqueness of weak limits, we conclude that the weak $L^2(0, T; \mathbf{L}^2(\Omega))$ limit ζ must coincide with the $L^1(0, T; \mathbf{L}^1(\Omega))$ limit. Consequently,

$$\frac{\tilde{\mu}(c_{\ell,n})}{K} \mathbf{u}_{\ell,n} \rightharpoonup \frac{\tilde{\mu}(c_\ell)}{K} \mathbf{u}_\ell \quad \text{weakly in } L^2(0, T; \mathbf{L}^2(\Omega)).$$

Now, we pass the limit in the equation (12), to conclude

$$\int_0^T \int_{\Omega} \frac{\tilde{\mu}(c_\ell)}{K} \mathbf{u}_\ell \cdot \mathbf{v} \eta(t) d\mathbf{x} dt + \int_0^T \int_{\Omega} (1 + \alpha c_\ell) \mathbf{g} \cdot \mathbf{v} \eta(t) d\mathbf{x} dt = 0,$$

for all $\mathbf{v} \in \mathbf{H}_m$ and $\eta \in C_c^\infty[0, T)$. Since this equation holds for all $m \in \mathbb{N}$, and the set $\bigcup_{m \geq 1} \mathbf{H}_m$ is dense in \mathbf{H} , the equality extends by a standard density argument to all $\mathbf{v} \in \mathbf{H}$. Finally, by the Fundamental Lemma of Calculus of Variations, this implies that the integrand must be zero for almost every $t > 0$:

$$\left(\frac{\tilde{\mu}(c_\ell(t))}{K} \mathbf{u}_\ell(t), \mathbf{v} \right) + ((1 + \alpha c_\ell(t)) \mathbf{g}, \mathbf{v}) = 0 \quad \forall \mathbf{v} \in \mathbf{H}, \quad \text{a.e. on } (0, \infty). \quad (13)$$

From Lemma 4.1, the sequence $\{c_{\ell,n} \mathbf{u}_{\ell,n}\}_n$ is uniformly bounded in $L^r(0, T; \mathbf{L}^2(\Omega))$, where $r = 2$ for $d = 2$ and $r = 4/3$ for $d = 3$. Consequently, there exists a subsequence (still denoted by $c_{\ell,n} \mathbf{u}_{\ell,n}$) that converges weakly to some limit ζ in $L^r(0, T; \mathbf{L}^2(\Omega))$. On the other hand, since $c_{\ell,n} \rightarrow c_\ell$ strongly in $L^2(0, T; \mathbf{L}^2(\Omega))$ and $\mathbf{u}_{\ell,n} \rightharpoonup \mathbf{u}_\ell$ weakly in $L^2(0, T; \mathbf{L}^2(\Omega))$, the product $c_{\ell,n} \mathbf{u}_{\ell,n} \rightharpoonup c_\ell \mathbf{u}_\ell$ in the $L^1((0, T); \mathbf{L}^1(\Omega))$ as $n \rightarrow \infty$. By the uniqueness of the weak limit, we identify $\zeta = c_\ell \mathbf{u}_\ell$. Equipped with these convergence results, we can pass to the limit in the discrete convection-diffusion equation (9). This establishes that for each fixed $\ell \in \mathbb{N}$, the pair $(c_\ell, \mathbf{u}_\ell)$ is a weak solution to the ℓ -approximate problem (5)-(6). \square

Next, we establish a maximum principle for the concentration c_ℓ . This result is crucial for deriving uniform bounds for the pair $\{(c_\ell, \mathbf{u}_\ell)\}_\ell$. Subsequently, utilizing weak and weak* compactness arguments, we extract a convergent subsequence and demonstrate that its limit as $\ell \rightarrow \infty$ constitutes a weak solution to the original problem.

Lemma 4.4 (Maximum Principle for Concentration). *Let $(c_\ell, \mathbf{u}_\ell)$ be a weak solution to the ℓ -approximate problem. Suppose the initial data satisfies $0 \leq c_0(\mathbf{x}) \leq M_2$ for almost every $\mathbf{x} \in \Omega$. Then, the concentration $c_\ell(t, \mathbf{x})$ satisfies*

$$0 \leq c_\ell(t, \mathbf{x}) \leq M_2, \quad \text{for almost every } (t, \mathbf{x}) \in (0, \infty) \times \Omega.$$

Proof. To establish the non-negativity of the concentration, we first define $\tilde{c}_\ell = \min\{0, c_\ell\}$. Substituting the test function $\phi = \tilde{c}_\ell$ into (6), we obtain

$$\frac{k+1}{2} \frac{d}{dt} \|\tilde{c}_\ell(t)\|_{L^2}^2 + (\mathbf{u}_\ell \cdot \nabla \tilde{c}_\ell, \tilde{c}_\ell) + D \|\nabla \tilde{c}_\ell(t)\|_{L^2}^2 + (\kappa \tilde{c}_\ell, \tilde{c}_\ell) = 0 \quad (14)$$

The second term on the left-hand side vanishes using integration by parts, with the continuity equation and boundary condition. Dropping the non-negative terms from the left-hand side of the above inequality and integrating in time from 0 to $\tau \in (0, \infty)$, we obtain

$$\|\tilde{c}_\ell(\tau)\|_{L^2}^2 \leq \|\tilde{c}_\ell(0)\|_{L^2}^2 = \|\tilde{c}(0)\|_{L^2}^2.$$

Since the initial data satisfies $c_0 \geq 0$, it follows that $\tilde{c}(0) = \min\{0, c_0\} = 0$. Consequently, we get $\|\tilde{c}(\tau)\| = 0$ for all $\tau \in (0, \infty)$, which implies that $c(t, \mathbf{x}) \geq 0$ for almost every $(t, \mathbf{x}) \in (0, \infty) \times \Omega$. Next, to prove c_ℓ is upper bounded we define $\tilde{c}_\ell = \max\{0, c_\ell - M_2\}$. Then, using $\phi = \tilde{c}$ as a test function in (6) we obtain

$$\frac{k+1}{2} \frac{d}{dt} \|\tilde{c}_\ell(t)\|_{L^2}^2 + (\mathbf{u}_\ell \cdot \nabla \tilde{c}_\ell, \tilde{c}_\ell) + D \|\nabla \tilde{c}_\ell\|_{L^2}^2 + (\kappa \tilde{c}_\ell, \tilde{c}_\ell) = 0.$$

Once again, the convection term vanishes due to integration by parts with the continuity equation and boundary conditions. Then dropping the non-negative terms from the left-hand side and integrating with respect to time from 0 to $t \in (0, \infty)$, we obtain:

$$\|\tilde{c}_\ell(t)\|_{L^2}^2 \leq \|\tilde{c}_\ell(0)\|_{L^2}^2 = \|\tilde{c}(0)\|_{L^2}^2, \quad \text{for all } t \in (0, \infty).$$

The initial data $c_0 \leq M_2$ implies $\tilde{c}(0) = \max\{0, c_0 - M_2\} = 0$. Using this in the above inequality, we get $\tilde{c}_\ell(t) = 0$ for all $t \in (0, \infty)$, which implies that $c_\ell(t, \mathbf{x}) \leq M_2$ a.e in $(0, \infty) \times \Omega$. This concludes the proof of the maximum principle. \square

Remark 1. *In the nonreactive case (i.e., $\kappa = 0$), if the initial data satisfies $0 < M_1 \leq c_0(\mathbf{x}) \leq M_2$ almost every $\mathbf{x} \in \Omega$, then the lower bound is preserved. Specifically, by employing the arguments of Lemma 4.4 with the test function $\tilde{c}_\ell = \min\{0, c_\ell - M_1\}$, one can show that*

$$c_\ell(t, \mathbf{x}) \geq M_1 \quad \text{for a.e. } (t, \mathbf{x}) \in (0, \infty) \times \Omega.$$

Proof of Theorem 4.1: Now, for each fixed $\ell \in \mathbb{N}$, let $(c_\ell, \mathbf{u}_\ell)$ be a solution to the ℓ -approximate problem. Lemma 4.4 along with the definition of $\tilde{\mu}$ gives

$$e^{-RM_2} \leq \tilde{\mu}(c_\ell) \leq e^{RM_2} \quad \text{a.e. on } (0, \infty) \times \Omega. \quad (15)$$

After revisiting the inequality (21) for \mathbf{u}_ℓ , we arrive at

$$\|\mathbf{u}_\ell\|_{L^p} \leq M \left\| \frac{K}{\tilde{\mu}(c_\ell)} (1 + \alpha c_\ell) \mathbf{g} \right\|_{L^p} \quad \text{for all } p \in [2, \infty).$$

A use of the Lemma 4.4 with (15) yields

$$\|\mathbf{u}_\ell\|_{L^p} \leq MK e^{-RM_2} (1 + \alpha M_2) \|\mathbf{g}\|_{L^\infty(\Omega)} |\Omega|, \quad \text{for all } p \in [2, \infty) \text{ and } \ell \in \mathbb{N}, \quad (16)$$

and hence, the sequence $\{\mathbf{u}_\ell\}_{\ell=1}^\infty$ is uniformly bounded in $L^\infty(0, T; \mathbf{L}^p(\Omega))$ for all $p \in [2, \infty)$. Now by repeating the arguments of Lemmas 4.1 and 4.2 for c_ℓ , and utilizing the bound $0 \leq c_\ell \leq M_2$, we obtain the following uniform estimates:

$$\|c_\ell\|_{L^\infty(0, T; L^\infty(\Omega))}, \|c_\ell\|_{L^2(0, T; H^1(\Omega))}, \left\| \frac{\partial c_\ell}{\partial t} \right\|_{L^2(0, T; (H^1)^*)} \leq M.$$

As before, using the uniform bounds and applying the Aubin–Lions lemma, we deduce that $c_\ell \rightarrow c$ strongly in $L^2(0, T; L^2(\Omega))$. Finally, we pass to the limit as $\ell \rightarrow \infty$ in equations (5) and (6) to establish that the limit pair (c, \mathbf{u}) is a solution to the original problem. Passing to the limit is straightforward for most terms, except for the viscosity term in the Darcy equation. To handle this term, we first prove that $\tilde{\mu}(c_\ell) \rightarrow \mu(c)$ strongly in $L^2(0, T; L^2(\Omega))$. By applying the triangle inequality, we obtain:

$$\|\tilde{\mu}(c_\ell) - \mu(c_\ell)\|_{L^2} \leq \|\tilde{\mu}(c_\ell) - \mu(c_\ell)\|_{L^2} + \|\mu(c_\ell) - \mu(c)\|_{L^2}. \quad (17)$$

Since $0 \leq c_\ell(t, \mathbf{x}) \leq M_2$ almost everywhere in $(0, T) \times \Omega$, the first term in the inequality above vanishes identically for any $\ell \geq M_2$. Moreover, because $c_\ell \rightarrow c$ in $L^2(0, T; L^2(\Omega))$ and μ is a Lipschitz function, it follows that $\mu(c_\ell) \rightarrow \mu(c)$ in $L^2(0, T; L^2(\Omega))$ as $\ell \rightarrow \infty$. Combining these results in inequality (17), we establish that $\tilde{\mu}(c_\ell) \rightarrow \mu(c)$ strongly in $L^2(0, T; L^2(\Omega))$. Next, since $\tilde{\mu}(c_\ell)$ is uniformly bounded in $L^\infty(0, T; L^\infty(\Omega))$, the product $\tilde{\mu}(c_\ell) \mathbf{u}_\ell$ is uniformly bounded in $L^2(0, T; L^2(\Omega))$. Consequently, there exists a subsequence such that $\tilde{\mu}(c_\ell) \mathbf{u}_\ell \rightharpoonup \zeta$ weakly in $L^2(0, T; L^2(\Omega))$. Since $\tilde{\mu}(c_\ell) \rightarrow \mu(c)$ strongly in $L^2(0, T; L^2(\Omega))$ and $\mathbf{u}_\ell \rightharpoonup \mathbf{u}$ weakly in $L^2(0, T; \mathbf{L}^2(\Omega))$, the product converges to $\mu(c) \mathbf{u}$ weakly in $L^1(0, T; \mathbf{L}^1(\Omega))$. By the uniqueness of weak limits, we identify $\zeta = \mu(c) \mathbf{u}$. With this convergence established, we pass to the limit $\ell \rightarrow \infty$ in equations (5) and (6), thereby concluding the proof of Theorem 4.1.

4.4 Uniqueness of Solution

In this section, we establish the uniqueness of weak solutions to the system (1a)–(1g). Recalling the estimate (11), we have

$$\|\mathbf{u}(t)\|_{L^p} \leq \left\| \frac{K}{\mu(c)} (1 + \alpha c) \mathbf{g} \right\|_{L^p} \quad \text{for } p \in [2, \infty).$$

Invoking the maximum principle (Lemma 4.4), which ensures $c \in L^\infty(0, T; L^\infty(\Omega))$, and using the lower bound $\mu(c) \geq 1$ together with $\mathbf{g} \in \mathbf{L}^\infty(\Omega)$, we deduce that $\mathbf{u} \in L^\infty(0, T; \mathbf{L}^p(\Omega))$ for all $p \in [2, \infty)$ and for $d \in \{2, 3\}$.

Theorem 4.2. *The problem (1) has at most one weak solution.*

Proof. Suppose not, let (c_i, \mathbf{u}_i) , $i = 1, 2$ be two weak solutions for the problem (1) satisfying (2)–(3) for $i = 1, 2$. On subtracting the resulting equations, it follows with $c = c_1 - c_2$ and $\mathbf{u} = \mathbf{u}_1 - \mathbf{u}_2$ that

$$\left(\frac{\mu(c_1(t))}{K} \mathbf{u}_1(t) - \frac{\mu(c_2(t))}{K} \mathbf{u}_2(t), \mathbf{v} \right) = (\alpha c(t) \mathbf{g}, \mathbf{v}), \quad \forall \mathbf{v} \in \mathbf{H}(\Omega), \quad (18)$$

and hence,

$$(k+1) \left\langle \frac{\partial c}{\partial t}, \phi \right\rangle + (c_1(t) \mathbf{u}_1(t) - c_2(t) \mathbf{u}_2(t), \nabla \phi) + D(\nabla(c_1(t) - c_2(t)), \nabla \phi) + (\kappa c(t), \phi) = 0. \quad (19)$$

Choose $\phi = c$ to obtain

$$\begin{aligned} \frac{(k+1)}{2} \frac{d}{dt} \|c(t)\|_{L^2}^2 + D\|\nabla c(t)\|_{L^2}^2 + (\kappa c(t), c(t)) &= -(c(t) \mathbf{u}_1(t), \nabla c(t)) - (c_2(t) \mathbf{u}(t), \nabla c(t)), \\ &= -\frac{1}{2} (\mathbf{u}_1(t), \nabla(c^2(t))) - (c_2(t) \mathbf{u}(t), \nabla c(t)). \end{aligned}$$

With the divergence theorem, the first term on the right-hand side vanishes. Then, an application of the Hölder's inequality to the second term yields

$$\frac{(k+1)}{2} \frac{d}{dt} \|c(t)\|_{L^2}^2 + D \|\nabla c(t)\|_{L^2}^2 \leq \|c_2(t)\|_{L^\infty(\Omega)} \|\mathbf{u}(t)\|_{L^2} \|\nabla c(t)\|_{L^2}. \quad (20)$$

Rearranging the left-hand side term of (18), it follows that

$$\left(\frac{\mu(c_1)}{K} (\mathbf{u}_1 - \mathbf{u}_2), \mathbf{v} \right) = - \left(\frac{1}{K} (\mu(c_1) - \mu(c_2)) \mathbf{u}_2, \mathbf{v} \right) + \alpha(c(t) \mathbf{g}, \mathbf{v}).$$

Now, setting $\mathbf{v} = \mathbf{u}(t)$ in the above equation, an application of the Holder's inequality shows

$$\frac{\mu_1}{K} \|\mathbf{u}(t)\|_{L^2}^2 \leq \frac{M}{K} \|c(t)\|_{L^4} \|\mathbf{u}_2\|_{L^4} \|\mathbf{u}\|_{L^2} + \alpha \|\mathbf{g}\|_{L^\infty(\Omega)} \|c(t)\|_{L^2} \|\mathbf{u}(t)\|_{L^2}.$$

A use of the Gagliardo-Nirenberg inequality yields

$$\|\mathbf{u}(t)\|_{L^2} \leq \frac{M}{\mu_1} \|\mathbf{u}_2(t)\|_{L^4} \|c(t)\|_{L^2}^{1-d/4} \|c(t)\|_{H^1}^{d/4} + \frac{\alpha K}{\mu_1} \|\mathbf{g}\|_{L^\infty(\Omega)} \|c(t)\|_{L^2}, \quad (21)$$

Using the estimate from inequality 21 in inequality 20, we obtain

$$\begin{aligned} \frac{1}{2} \frac{d}{dt} \|c(t)\|_{L^2}^2 + D \|\nabla c(t)\|_{L^2}^2 &\leq \frac{M}{\mu_1} \|\mathbf{u}_2(t)\|_{L^4} \|c_2(t)\|_{L^\infty(\Omega)} \|c(t)\|_{L^2}^{1-d/4} \|c(t)\|_{H^1}^{d/4} \|\nabla c(t)\|_{L^2} \\ &\quad + \frac{\alpha K}{\mu_1} \|c_2(t)\|_{L^\infty(\Omega)} \|\mathbf{g}\|_{L^\infty(\Omega)} \|c(t)\|_{L^2} \|\nabla c(t)\|_{L^2} + \|\kappa\|_{L^\infty(\Omega)} \|c(t)\|_{L^2}^2. \end{aligned}$$

An application of Young's inequality shows

$$\begin{aligned} \frac{1}{2} \frac{d}{dt} \|c(t)\|_{L^2}^2 + D \|\nabla c(t)\|_{L^2}^2 &\leq \epsilon \|\nabla c(t)\|_{L^2}^2 + \epsilon \|c(t)\|_{H^1}^2 + M_\epsilon \|\mathbf{u}_2(t)\|_{L^4}^{8/(4-d)} \|c_2(t)\|_{L^\infty(\Omega)}^{8/(4-d)} \|c(t)\|_{L^2}^2 \\ &\quad + \epsilon \|\nabla c(t)\|_{L^2}^2 + K_\epsilon \|c_2(t)\|_{L^\infty(\Omega)}^2 \|\mathbf{g}\|_{L^\infty(\Omega)}^2 \|c(t)\|_{L^2}^2 + \|\kappa\|_{L^\infty(\Omega)} \|c(t)\|_{L^2}^2. \end{aligned}$$

Define $M_\epsilon = \max \{M_\epsilon, K_\epsilon\}$ and set $\phi(t) = \|c_2(t)\|_{L^\infty(\Omega)}^{8/(4-d)} \|\mathbf{u}_2(t)\|_{L^4}^{8/(4-d)} + \|c_2(t)\|_{L^\infty(\Omega)}^2 \|\mathbf{g}\|_{L^\infty(\Omega)}^2 + \|\kappa\|_{L^\infty(\Omega)} \|c(t)\|_{L^2}^2 + \epsilon$. Then we arrive at

$$\frac{1}{2} \frac{d}{dt} \|c(t)\|_{L^2}^2 + (D - 3\epsilon) \|\nabla c(t)\|_{L^2}^2 \leq M_\epsilon \phi(t) \|c(t)\|_{L^2}^2.$$

Choose $\epsilon > 0$ sufficiently small with $\epsilon < \frac{D}{3}$. Then, an application of the Grönwall's inequality yields

$$\|c_1(t) - c_2(t)\|_{L^2} \leq \|c_1(0) - c_2(0)\|_{L^2} e^{M \int_0^\infty \phi(s) ds}, \quad \text{for } t \in (0, \infty). \quad (22)$$

Since $\phi \in L^1(0, \infty)$ and $c_1(0) - c_2(0) = 0$. Substituting this into the preceding inequality, it follows that $c_1(t, \mathbf{x}) = c_2(t, \mathbf{x})$ for almost every $(t, \mathbf{x}) \in (0, \infty) \times \Omega$. Using the equality $c_1 = c_2$ in inequality 21, we further deduce that $\mathbf{u}_1(t, \mathbf{x}) = \mathbf{u}_2(t, \mathbf{x})$ for almost every $(t, \mathbf{x}) \in (0, \infty) \times \Omega$. This completes the rest of the proof. \square

5 Asymptotic Behavior as $t \rightarrow \infty$

This section deals with asymptotic behaviour of the concentration c as $t \rightarrow \infty$.

Theorem 5.1. *Suppose (c, \mathbf{u}) is a solution to the system (1). Then there exist constants $C_p > 0$ and $\lambda > 0$ such that for all $t \geq 0$:*

$$\|c(t)\|_{L^p(\Omega)} \leq C_p e^{-\alpha t} \|c_0\|_{L^p(\Omega)}, \quad \forall p \in [1, \infty].$$

Proof. By choosing $\phi = 1$ as a test function in (3), the diffusion and convection terms vanish due to the divergence-free constraint and boundary conditions, yielding

$$\begin{aligned} (1+k) \int_\Omega \frac{\partial c}{\partial t} dx &= - \int_\Omega \kappa c(t) dx, \\ &\geq -\kappa_1 \int_\Omega c(t) dx, \end{aligned}$$

since $c \geq 0$ and $\kappa \geq \kappa_1 > 0$. The above inequality can be rewritten as the following differential inequality:

$$(k+1) \frac{d}{dt} \|c(t)\|_{L^1} \leq -\kappa_1 \|c(t)\|_{L^1}, \quad \text{for all } t \geq 0.$$

An application of Grönwall's inequality yields

$$\|c(t)\|_{L^1} \leq \|c(0)\|_{L^1} e^{-\frac{\kappa_1}{k+1} t}, \quad \text{for all } t \geq 0. \quad (23)$$

This implies that the spatial average concentration converges to zero as $t \rightarrow \infty$.

Now to prove exponential convergence in L^∞ -norm, let $\lambda = \frac{\kappa_1}{k+1}$ and define the auxiliary function $w(t, \mathbf{x}) = e^{\lambda t} c(t, \mathbf{x})$. A direct substitution of $c = w e^{-\lambda t}$ into equation (3) shows

$$(k+1) \langle \frac{\partial w}{\partial t} - \lambda w, \phi \rangle + (w \mathbf{u}, \nabla \phi) + D(\nabla w, \nabla \phi) + (\kappa w, \phi) = 0.$$

Rearranging and using $\lambda(k+1) = \kappa_1$, we arrive at

$$(k+1) \langle \frac{\partial w}{\partial t}, \phi \rangle + (w \mathbf{u}, \nabla \phi) + D(\nabla w, \nabla \phi) + ((\kappa - \kappa_1)w, \phi) = 0.$$

Now using the test function $\phi = \max\{0, \|w(0)\|_{L^\infty}\}$ and following the similar arguments as in Lemma 4.4, we conclude

$$\|w(t)\|_{L^\infty(\Omega)} \leq \|w(0)\|_{L^\infty(\Omega)} = \|c(0)\|_{L^\infty(\Omega)}.$$

Substituting back the definition of w , gives the following exponential decay estimate in the L^∞ norm:

$$\|c(t)\|_{L^\infty(\Omega)} \leq \|c(0)\|_{L^\infty(\Omega)} e^{-\frac{\kappa_1}{k+1} t}. \quad (24)$$

Finally, to obtain the L^p decay estimates, we employ the interpolation inequality for $p \in (1, \infty)$:

$$\|c(t)\|_{L^p} \leq \|c(t)\|_{L^1}^{1/p} \|c(t)\|_{L^\infty}^{1-1/p}.$$

Now, we use the decay estimates from (23) and (24):

$$\begin{aligned} \|c(t)\|_{L^p} &\leq \left(\|c(0)\|_{L^1} e^{-\frac{\kappa_1}{k+1} t} \right)^{1/p} \left(\|c(0)\|_{L^\infty(\Omega)} e^{-\frac{\kappa_1}{k+1} t} \right)^{1/q} \\ &= \|c(0)\|_{L^1}^{1/p} \|c(0)\|_{L^\infty}^{1/q} e^{-\frac{\kappa_1}{k+1} (\frac{1}{p} + \frac{1}{q}) t} \\ &= \|c(0)\|_{L^1}^{1/p} \|c(0)\|_{L^\infty}^{1/q} e^{-\frac{\kappa_1}{k+1} t}. \end{aligned}$$

This completes the proof of the Theorem. \square

6 Numerical Results and Discussion

This section presents a detailed numerical study of the initial-boundary value problem (1).

Our numerical study is divided into two parts. First, in Subsections 6.1 through 6.4, we consider the non-reactive case by setting $\kappa = 0$. This allows us to isolate the effects of the viscosity contrast (R), density contrast (α), and adsorption coefficient (k) on instability and mixing behavior. In Subsection 6.5, we introduce the reaction terms and specifically discuss how the reaction coefficient (κ) and the adsorption coefficient (k) modulate the exponential decay rate. To align with our analytical framework, the concentration-dependent viscosity is specifically chosen as an exponential function of the form $\mu(c) = e^{Rc}$, where R is the viscosity contrast coefficient. The purpose of this investigation is to validate the theoretical findings and to illustrate the qualitative behavior of the solutions. The problem is studied in the space-time domain $(0, T) \times \Omega$, with $\Omega = \{(x, y) \in \mathbb{R}^2 \mid x \in (0, 100), y \in (0, 200)\}$ representing a rectangular region, and $T > 0$, the duration of the simulation. We reformulate the system by applying the divergence operator to Darcy's law (1b), and utilizing the mass conservation equation (1a), thus eliminating the velocity variable from the system. This reformulation enables us to solve for pressure and concentration alone, while the velocity field can be subsequently recovered using Darcy's law (1b). The weak formulation corresponding to this system is given by:

$$0 = \int_{\Omega} e^{-Rc} (\nabla p + (1 + \alpha c) \mathbf{g}) \cdot \nabla q, \quad (25a)$$

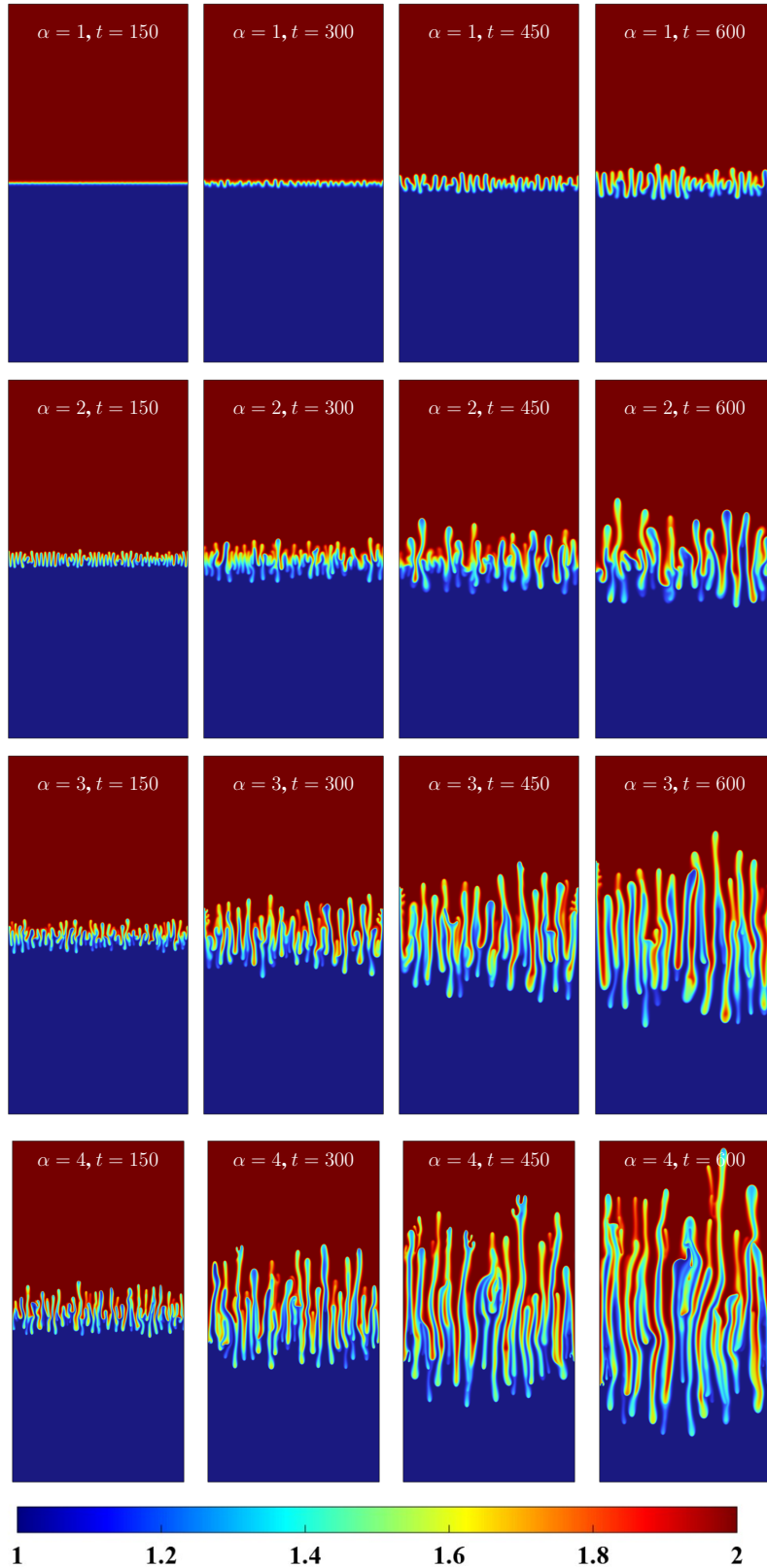


Figure 1: Time evolution of concentration profiles at $t = 150, 300, 450, 600$ (left to right) for $\alpha = 1, 2, 3, 4$ (top to bottom).

$$0 = \int_{\Omega} -\frac{\partial c}{\partial t} \phi + c e^{-Rc} (\nabla p + (1 + \alpha c) \mathbf{g}) \cdot \nabla \phi - D \nabla c \cdot \nabla \phi. \quad (25b)$$

Here, q and ϕ are test functions corresponding to the pressure and concentration, respectively. No-flux boundary conditions are imposed. The initial distribution of the concentration is given by:

$$c(0, x, y) = \begin{cases} 2, & y \geq 100, \\ 1, & y < 100. \end{cases} \quad (26)$$

The weak formulation (25) is solved using the finite element method in COMSOL MULTIPHYSICS® [6], with $D = 0.005$ and for various values of the density contrast coefficient α , adsorption coefficient k , and viscosity contrast R . Free quadrilateral elements were used for the spatial discretizations. A random perturbation of magnitude 10^{-3} was applied at the interface in the initial concentration field to trigger the instability. The same random seed was used for all simulations to maintain consistency in the perturbation pattern. To quantify the instability, we compute the total kinetic energy defined as $\int_{\Omega} (u^2 + v^2)$, where u and v are the velocity components. To evaluate the mixing, we used the degree of mixing. These quantities are computed for various parameter values of α , k , and R , to analyze the effects of viscosity contrast, adsorption, and density contrast on both the instability and the mixing dynamics.

6.1 Total kinetic energy

The total kinetic energy of this system is given by

$$\mathcal{E}(t) = \int_{\Omega} (u^2 + v^2) dx dy.$$

Using test function $\mathbf{v} = \mathbf{u}(t)$, and Holder's inequality in equation (3), we get

$$\|\mathbf{u}(t)\|_{L^2}^2 \leq e^{-2R} \|1 + \alpha c(t)\|_{L^2}^2.$$

Using the triangle inequality and the fact that $\|c(t)\|_{L^2} \leq \|c_0\|_{L^2}$, we obtain

$$\mathcal{E}(t) = \|\mathbf{u}(t)\|_{L^2}^2 \leq e^{-2R} \left(\alpha^2 + \frac{6}{5}\alpha + \frac{2}{5} \right) \|c_0\|_{L^2}^2. \quad (27)$$

From the above inequality, we observe that an increase in R leads to a decrease in energy, indicating a flow stabilization. In contrast, as α increases, the energy also increases, suggesting an improvement in flow dynamics. This implies that the instability intensifies with increasing α and decreases as R increases.

6.2 Degree of Mixing

The degree of mixing is a quantitative metric that characterizes the extent of homogeneity of a scalar field, such as concentration, temperature, or density, within a specified domain. Following Jha et al. [14], we quantify the mixing efficiency using the normalized variance of the concentration field. From the estimate in (29), we have $\sigma_c^2(t) \leq \sigma_c^2(0)$ for all $t \in [0, T]$, we set the maximum variance as $\sigma_{\max}^2 = \sigma_c^2(0)$. Consequently, the degree of mixing $\chi(t)$ is defined as

$$\chi(t) = 1 - \frac{\sigma_c^2(t)}{\sigma_c^2(0)}, \quad (28)$$

where $\sigma_c^2(t)$ represents the spatial variance at time t , given by

$$\sigma_c^2(t) = \frac{1}{|\Omega|} \int_{\Omega} (c - \bar{c})^2 dx dy.$$

Here, \bar{c} denotes the average concentration and $|\Omega|$ is the area of the domain Ω .

In equation (3), by setting $\phi = 1$, we can demonstrate that the total concentration remains conserved, meaning it retains its initial value. Specifically, it remains constant over time:

$$\bar{c}(t) = \frac{1}{|\Omega|} \int_{\Omega} c(t, x, y) dx dy = \frac{1}{|\Omega|} \int_{\Omega} c(0, x, y) dx dy.$$

Furthermore, by choosing the test function $\phi = c(t) - \bar{c}$ in convection diffusion equation, we obtain

$$\frac{(1+k)}{2} \frac{d}{dt} \|c(t) - \bar{c}\|_{L^2}^2 + \int_{\Omega} \mathbf{u}(t) \cdot \nabla (c(t) - \bar{c})(c(t) - \bar{c}) dx dy + D \|\nabla (c(t) - \bar{c})\|_{L^2}^2 = 0$$

Applying integration by parts and using the no-flux boundary conditions, the second term in the above equation vanishes. Furthermore, by applying Poincaré's inequality, we obtain

$$\|c - \bar{c}\|_{L^2} \leq M \|\nabla(c - \bar{c})\|_{L^2},$$

where M is the Poincaré constant. For a rectangular domain $\Omega = (0, L_x) \times (0, L_y)$, the optimal Poincaré constant is: $M = \frac{1}{\pi} \cdot \max\{L_x, L_y\}$. With these observations, the above equation simplifies to

$$\frac{d}{dt} \|c(t) - \bar{c}\|_{L^2}^2 + \frac{2D}{M(1+k)} \|c(t) - \bar{c}\|_{L^2}^2 \leq 0,$$

and hence,

$$\|c(t) - \bar{c}\|_{L^2}^2 \leq \|c_0 - \bar{c}\|_{L^2}^2 e^{-\frac{2D}{M(1+k)} t}.$$

From the definition of variance, we can write

$$0 \leq \frac{\sigma_c^2(t)}{\sigma_c^2(0)} \leq e^{-\frac{2D}{M(1+k)} t}. \quad (29)$$

From the above inequality, we observe that the variance is maximum at $t = 0$ and decreases over time, with $\sigma_c^2(t) \rightarrow 0$ as $t \rightarrow \infty$. This relationship can be reformulated in terms of the degree of mixing.

$$1 - e^{-\frac{2D}{M(1+k)} t} \leq \chi(t) \leq 1 \quad (30)$$

From the last inequality, we observe that $\chi(t) \in [0, 1]$ for all times, with $\chi(0) = 0$ and $\chi(t) \rightarrow 1$ as $t \rightarrow \infty$. The degree of mixing quantifies the degree of homogeneity: values close to zero indicate minimal mixing, while a higher value means increased mixing, reaching complete mixing when $\chi(t) = 1$. Furthermore, we observe that the mixing process slows down as the parameter k increases.

6.3 Mesh Convergence Study

Mesh size h	DOF	Energy Error		Variance Error	
		$\ E_h - E_{\text{ref}}\ _{L^\infty}$	$\frac{\ E_h - E_{\text{ref}}\ _{L^2}}{\ E_{\text{ref}}\ _{L^2}}$	$\frac{\ \text{Var}_h - \text{Var}_{\text{ref}}\ _{L^\infty}}{\ \text{Var}_{\text{ref}}\ _{L^\infty}}$	$\frac{\ \text{Var}_h - \text{Var}_{\text{ref}}\ _{L^2}}{\ \text{Var}_{\text{ref}}\ _{L^2}}$
0.640000	395010	0.1837	0.3301	0.0091	0.0041
0.327680	1494506	0.0646	0.1177	0.0026	0.0013
0.262144	2336310	0.0328	0.0511	0.0007	0.0002

Table 1: Error in energy and variance for different mesh sizes, in L^2 and L^∞ norms

A well-chosen mesh can provide higher accuracy while reducing computational expense. To ensure the independence of the numerical solution mesh, we performed a refinement study by varying the maximum element size h from the set $\{0.64, 0.327680, 0.262144, 0.16777\}$. For this test, the model parameters are fixed as $R = 2$, $\alpha = 2$, $k = 2$, and the diffusion coefficient $d = 0.005$. The finest mesh, corresponding to $h = 0.16777$, is considered the reference solution. To quantify mesh convergence, we compute the relative error in two physical quantities of interest: the total kinetic energy and the degree of mixing. Total kinetic energy serves as a quantitative indicator of the growth of the fingering instability [18], while the degree of mixing measures the extent of concentration homogenization in the domain. These metrics are chosen because of their relevance in characterizing the evolution of instability and mixing in porous media flows. Here, E_h and Var_h denote the computed total kinetic energy and variance, respectively, on a mesh with maximum element size h , while E_{ref} and Var_{ref} denote the corresponding reference values computed on the finest mesh with $h = 0.16777$. Table 1 presents the errors in total kinetic energy and variance for various mesh sizes h , measured in the L^2 and L^∞ norms. As the total kinetic energy is nearly zero at early times, absolute error is used instead of relative error to ensure meaningful comparisons. As seen in Table 1, the errors decrease consistently with decreasing h , demonstrating numerical convergence. The smallest errors occur at $h = 0.262144$; thus, this mesh size is used for all subsequent simulations. Our theoretical investigation has determined both the upper and lower bounds for the concentration and demonstrated that the system complies with the principles of mass conservation for the concentration. Numerical simulations verify that the applied numerical method meets these theoretical bounds and ensures total mass conservation with high precision, thus affirming the accuracy of the numerical method employed.

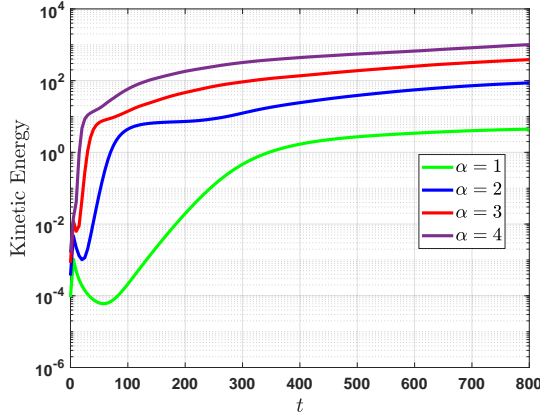


Figure 2: Energy evolution over time for different values of α , with $k = 1$ and $R = 1$.

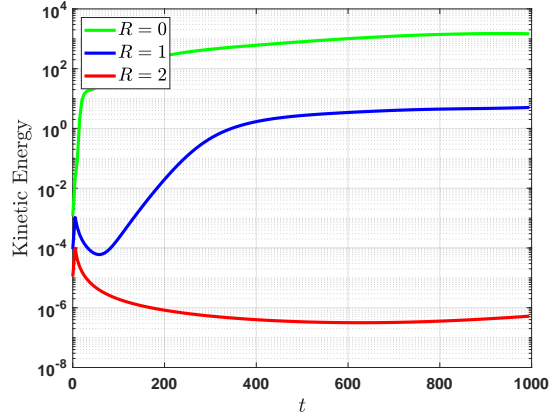


Figure 3: Energy evolution over time for different values of R , with $\alpha = 1$ and $k = 1$.

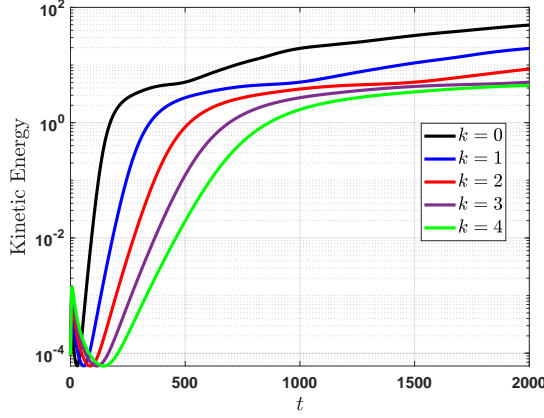


Figure 4: Energy evolution over time for different values of k , with $\alpha = 1$ and $R = 1$.

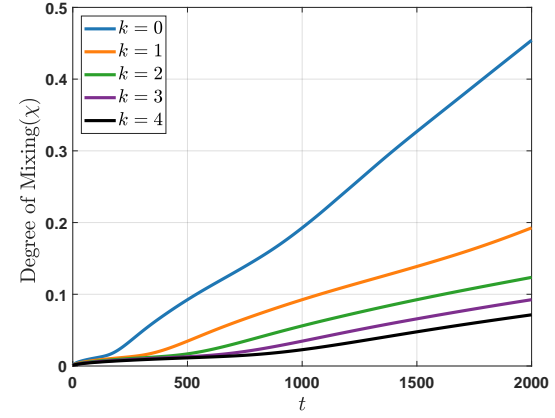


Figure 5: Variation of the degree of mixing over time for different values of k , with $\alpha = 1$ and $R = 1$.

6.4 Instability and Mixing Behavior under Adsorption, Viscosity, and Density Variations

Spatio-temporal evolution of the concentration profile for $k = 1$ and $R = 1$ at $t = 150, 300, 450$, and 600 (columns), for $\alpha = 1, 2, 3$, and 4 (rows), is shown in Figure 1. From inequality (27), it is evident that the total kinetic energy increases with increasing α , indicating enhanced flow activity. This trend is also clearly illustrated in Figure 1. Let \mathcal{E}_α denote the total kinetic energy corresponding to the parameter α . From inequality (27), we find $\mathcal{E}_{\alpha=2} \geq 2.61 \mathcal{E}_{\alpha=1}$, $\mathcal{E}_{\alpha=3} \geq 1.91 \mathcal{E}_{\alpha=2}$, and $\mathcal{E}_{\alpha=4} \geq 1.63 \mathcal{E}_{\alpha=3}$. This shows that the energy increase from $\alpha = 1$ to $\alpha = 2$ is the largest, with progressively smaller relative increases for $\alpha = 2 \rightarrow 3$ and $\alpha = 3 \rightarrow 4$. A similar pattern is observed in Figure 2.

As the adsorption parameter k increases, a noticeable suppression of the instability is observed, suggesting that stronger adsorption leads to a more stabilized flow. To quantify this effect, we plot the evolution of total kinetic energy over time in Figure 4 for different values of $k = 0, 1, 2, 3, 4$. The results are consistent: energy decreases as the value of k increases, further confirming the stabilizing influence of adsorption. In addition to analyzing instability, we plot the degree of mixing for different values of $k = 0, 1, 2, 3, 4$ to track the mixing process. As evident from equation (30), the degree of mixing satisfies the approximate bounds $\chi_{k=0} \gtrsim 2\chi_{k=1}$, $\chi_{k=1} \gtrsim 1.5\chi_{k=2}$, $\chi_{k=2} \gtrsim 1.33\chi_{k=3}$ and $\chi_{k=3} \gtrsim 1.24\chi_{k=4}$, suggesting that the influence of the parameter k on mixing becomes progressively weaker as k increases. This trend is further confirmed by the corresponding plot 5, which clearly illustrates the decreasing sensitivity of the degree of mixing with increasing k .

As indicated by inequality (27), a significant energy reduction is observed as the value of R increases. This trend is corroborated by Figure 3, which illustrates a temporal decline in energy at elevated R values. For example, the scenario corresponding to $R = 0$ displays specific energy levels, whereas for $R = 1$, the energy remains minimal, and for $R = 2$, the flow is comparatively stable.

6.5 Numerical Study of Exponential Decay in the Reactive Case

In this section, we numerically investigate the impact of the adsorption coefficient k and the reaction constant κ on the exponential decay of the concentration, fixing $\alpha = 1$ and $R = 1$. Setting $\kappa_1 = \kappa_2 = \kappa$ in Theorem 5.1, we obtain the theoretical exponential decay rate $\lambda = \frac{2\kappa}{k+1}$ for the concentration in the L^p norm, where $p \in [1, \infty]$. We compare this theoretical rate λ with the numerical decay rate $\tilde{\lambda}$ obtained from simulations for the L^2 norm ($p = 2$).

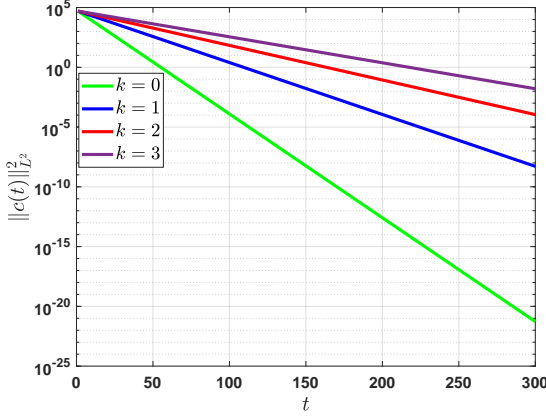


Figure 6: Log-linear plot of $\|c(t)\|_{L^2}^2$ decay versus time for $k = 0, 1, 2, 3$, at a fixed $\kappa = 0.1$.

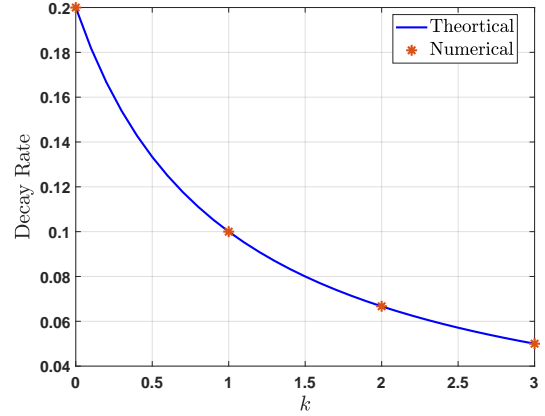


Figure 7: Theoretical decay rate, $\lambda = 0.2/(k+1)$, compared against the numerically computed decay rates (dots) for $k = 0, 1, 2, 3$.

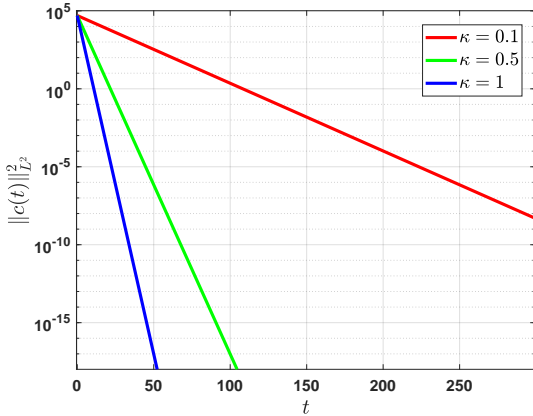


Figure 8: Log-linear plot of $\|c(t)\|_{L^2}^2$ decay versus time for $\kappa = 0.1, 0.5, 1$, at a fixed $k = 1$.

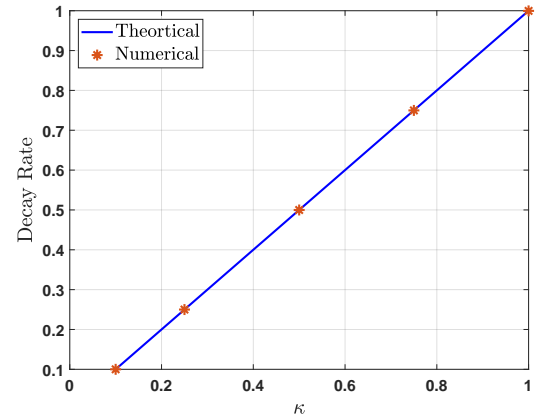


Figure 9: Theoretical decay rate, $\lambda = \kappa$, compared against the numerically computed decay rates (dots) for $\kappa = 0.1, 0.25, 0.5, 0.75, 1$.

Effect of the Adsorption Coefficient (k): First, we fix $\kappa = 0.1$ and vary $k \in \{0, 1, 2, 3\}$. Figure 6 plots $\|c(t)\|_{L^2}^2$ versus time using a logarithmic scale for the y-axis. We clearly observe exponential decay, where the slope of the lines represents the numerical decay rate. This figure matches the theoretical qualitative behavior: as k increases, the

slope of the lines decreases, indicating a slower decay rate. We then compute the numerical decay rate $\tilde{\lambda}$ using an exponential MATLAB fit. In Figure 7, we plot both the numerical ($\tilde{\lambda}$) and theoretical (λ) decay rates as a function of k . The results show an excellent match.

Effect of the Reaction Constant (κ): Next, we fix $k = 1$, which simplifies the theoretical decay rate to $\lambda = \kappa$. We then test $\kappa \in \{0.1, 0.5, 1\}$. As predicted, a larger κ leads to a faster decay rate. This qualitative behavior is observed in Figure 8, which plots $\|c(t)\|_{L^2}^2$ vs. time for these κ values. As with the k -study, a comparison of the theoretical and numerical decay rates as a function of κ is shown in Figure 9, showing an excellent match.

7 Concluding Remarks

In this work, we have rigorously investigated a generalized mathematical model for density-driven flow in porous media, incorporating the coupled effects of linear adsorption and concentration-dependent viscosity. We established the well-posedness of the system by proving the existence, uniqueness, and continuous dependence on initial data of weak solutions in both two and three spatial dimensions. The physical consistency of the model was further confirmed through the establishment of maximum and minimum principles, ensuring the boundedness and non-negativity of the concentration field. Furthermore, our analytical results demonstrate that the concentration converges exponentially to zero in the L^p -norm for all $1 \leq p \leq \infty$ as $t \rightarrow \infty$, providing a definitive asymptotic limit for the mixing process.

To validate these theoretical findings, we implemented a numerical framework based on a pressure formulation that eliminates the velocity variable to reduce computational complexity. This approach, implemented via the finite element method in COMSOL Multiphysics, offers a significant advantage over traditional stream-vorticity formulations by remaining applicable to three-dimensional domains. The numerical simulations closely align with the qualitative behavior predicted by our analytical results. Specifically, while increasing the density contrast intensifies finger-like structures and enhances the total kinetic energy, the results reveal a clear saturation effect. The growth in total kinetic energy is most pronounced at lower ranges of the density contrast and exhibits diminishing marginal increments as the contrast continues to rise, a nonlinear sensitivity that is consistent with our theoretical energy estimates. Furthermore, the simulations confirm that increasing the adsorption coefficient suppresses mixing efficiency; however, the rate of reduction in mixing weakens as the coefficient increases, further validating our theoretical predictions regarding the damping effect provided by the porous matrix.

These findings highlight the complex, nonlinear interplay between adsorption and hydrodynamic instability. Future work will address the analytical challenges introduced by nonlinear adsorption isotherms (e.g., Langmuir or Freundlich), which complicate the derivation of global energy bounds. Additionally, we aim to extend the current well-posedness framework to spatially heterogeneous media, where discontinuous permeability coefficients present new difficulties for regularity theory.

References

- [1] S. Al-Hajri, S. M. Mahmood, H. Abdulelah, and S. Akbari. An Overview on Polymer Retention in Porous Media. *Energies*, 11(10):2751, 2018.
- [2] K. Allali, V. Volpert, and V. Vougalter. A model of miscible liquids in porous media. *Electron. J. Differ. Equ.*, 264:1–10, 2015.
- [3] C. Almarcha, P. M. J. Trevelyan, P. Grosfils, and A. De Wit. Chemically Driven Hydrodynamic Instabilities. *Phys. Rev. Lett.*, 104(4):044501, 2010.
- [4] Y. Amirat and V. Shelukhin. Global Weak Solutions to Equations of Compressible Miscible Flows in Porous Media. *SIAM J. Math. Anal.*, 38(6):1825–1846, 2007.
- [5] Z. Chen and R. E. Ewing. Mathematical Analysis for Reservoir Models. *SIAM J. Math. Anal.*, 30(2):431–453, 1999.
- [6] COMSOL AB. *COMSOL Multiphysics® v. 6.2*. COMSOL AB, Stockholm, Sweden, 2024. <https://www.comsol.com>.
- [7] D. Daniel and A. Riaz. Effect of viscosity contrast on gravitationally unstable diffusive layers in porous media. *Phys. Fluids*, 26(11):116601, 2014.
- [8] B. L. Darlow, R. E. Ewing, and M. F. Wheeler. Mixed finite element method for miscible displacement problems in porous media. *Soc. Pet. Eng. J.*, 24(04):391–398, 1984.
- [9] W. H. Van der Molen and H. C. Van Ommen. Transport of solutes in soils and aquifers. *J. Hydrol.*, 100(1–3):433–451, 1988.

[10] M. Ebenbeck and H. Garcke. On a Cahn–Hilliard–Brinkman Model for tumor growth and its singular limits. *SIAM J. Math. Anal.*, 51(3):1868–1912, 2017.

[11] G. Di Fazio. l^p estimates for divergence form elliptic equations with discontinuous coefficients. *Boll. Un. Mat. Ital. A* (7), 10(2):409–420, 1996.

[12] T. K. Hota, S. Pramanik, and M. Mishra. Onset of fingering instability in a finite slice of adsorbed solute. *Phys. Rev. E*, 92(2):023013, 2015.

[13] H. E. Huppert and J. A. Neufeld. The fluid mechanics of carbon dioxide sequestration. *Annu. Rev. Fluid Mech.*, 46:255–272, 2014.

[14] B. Jha, L. Cueto-Felgueroso, and R. Juanes. Fluid mixing from viscous fingering. *Phys. Rev. Lett.*, 106(19):194502, 2011.

[15] W. J. Weber Jr, P. M. McGinley, and L. E. Katz. Sorption phenomena in subsurface systems: concepts, models and effects on contaminant fate and transport. *Water Res.*, 25(5):499–528, 1991.

[16] P. H. Krumrine, J. S. Falcone, and T. C. Campbell. Surfactant flooding 1: the effect of alkaline additives on IFT, surfactant adsorption, and recovery efficiency. *Soc. Pet. Eng. J.*, 22(04):503–513, 1982.

[17] S. Kundu, S. N. Maharana, and M. Mishra. Existence and uniqueness of solution to unsteady Darcy–Brinkman problem with Korteweg stress for modelling miscible porous media flow. *J. Math. Anal. Appl.*, 539(2):128532, 2024.

[18] T. Lyubimova, A. Vorobev, and S. Prokopev. Rayleigh–Taylor instability of a miscible interface in a confined domain. *Phys. Fluids*, 31(1):014104, 2019.

[19] O. Manickam and G. M. Homsy. Fingering instabilities in vertical miscible displacement flows in porous media. *J. Fluid Mech.*, 288:75–102, 1995.

[20] K. J. Mayfield, R. A. Shalliker, H. J. Catchpoole, A. P. Sweeney, V. Wong, and G. Guiochon. Viscous fingering induced flow instability in multidimensional liquid chromatography. *J. Chromatogr. A*, 1080(2):124–131, 2005.

[21] S. Pramanik and M. Mishra. Coupled effect of viscosity and density gradients on fingering instabilities of a miscible slice in porous media. *Phys. Fluids*, 28(8):084104, 2016.

[22] S. Pramanik, A. De Wit, and M. Mishra. Viscous fingering and deformation of a miscible circular blob in a rectilinear displacement in porous media. *J. Fluid Mech.*, 782:R2, 2015.

[23] C. Rana and M. Mishra. Fingering dynamics on the adsorbed solute with influence of less viscous and strong sample solvent. *J. Chem. Phys.*, 141(21):214701, 2014.

[24] C. Rana, S. Pramanik, M. Martin, A. De Wit, and M. Mishra. Influence of Langmuir adsorption and viscous fingering on transport of finite size samples in porous media. *Phys. Rev. Fluids*, 4(10):104001, 2019.

[25] Rayleigh. Investigation of the character of the equilibrium of an incompressible heavy fluid of variable density. *Proc. Lond. Math. Soc.*, s1-14(1):170–177, 1882.

[26] A. Sayari and Y. Belmabkhout. Stabilization of amine-containing CO_2 adsorbents: dramatic effect of water vapor. *J. Am. Chem. Soc.*, 132(18):6312–6314, 2010.

[27] R. A. Shalliker, H. J. Catchpoole, G. R. Dennis, and G. Guiochon. Visualising viscous fingering in chromatography columns: High viscosity solute plug. *J. Chromatogr. A*, 1142(1):48–55, 2007.

[28] M. Stanislaw and P. Szafraniec. Nonmonotone slip problem for miscible liquids. *J. Math. Anal. Appl.*, 471:342–357, 2019.

[29] G. I. Taylor. The instability of liquid surfaces when accelerated in a direction perpendicular to their planes. I. *Proc. R. Soc. Lond. A Math. Phys. Sci.*, 201(1065):192–196, 1950.

[30] Y. Wei. Stabilized finite element methods for miscible displacement in porous media. *ESAIM Math. Model. Numer. Anal.*, 28(5):611–665, 1994.

[31] D. Zhang, T. Liu, and V. Prigobbe. Enhanced solute transport in porous media due to pH-dependent adsorption and transverse dispersion. *Adv. Water Resour.*, 164:104195, 2022.